2012 12th International Conference on Control, Automation and Systems
Oct. 17-21, 2012 in ICC, Jeju Island, Korea

Tool-Point Control of a Planar Hydraulically Actuated Manipulator with Compensation of Non-Actuated Degree of Freedom

Magnus B. Kjelland[1], Michael R. Hansen[1],Ilya Tyapin[1] and Geir Hovland[1]

[1]Department of Engineering, University of Agder, Grimstad, Norway
(Tel : +47 37 23 30 00; E-mail:(magnus.b.kjelland, michael.r.hansen, ilya.tyapin, geir.hovland)@ uia.no))

Abstract: The current work is on motion control of a hydraulically actuated manipulator with a view to handle offshore payload transfer between moving frames. The manipulator has redundant actuation and also, a non-actuated degree of freedom. The motion control has two targets: tool point control and compensation of the non-actuated degree of freedom. The redundancy is handled by means of pseudo-inverse kinematics while optimizing a cost function, avoiding mechanical joint limits. The compensation of the un-actuated degree of freedom employs LQR control, minimizing position and velocity error while maintaining the tracking reference for the tool-point. The proposed control scheme is implemented and experimentally validated in a practical system where the manipulator is mounted on a Stewart platform that allows for the simulation of wave induced heave motion as a disturbance.

Keywords: End Point Control, Active Compensation, Electro-Hydraulic Systems, Redundant Manipulators, Sensors.

1. INTRODUCTION

In offshore applications there is a wide variety of tool point control tasks related to heave compensation. This is the case in offshore areas such as oil and gas, ship transportation and in offshore wind power systems, where disturbances from sea waves represent a significant challenge for any type of payload manipulation. Machines that handle heavy objects, such as hanging loads, are greatly affected by the ocean environment, and in order to maintain an acceptable performance in as rough weather as possible active heave compensation is widely used.

For hanging loads the main objective of the heave compensation is to control the velocity of the payload mass center relatve to either an inertial or moving frame depending on the nature of the source and target of the payload transfer. This will lead to an increased weather window of operation and reduced dynamic loading on both structures and actuation system.

Controlling the velocity relative to a frame can always be converted to a tool point control problem if both the source and the target frame are known relative to a common frame. Within offshore applications sensor systems, typically referred to as M(otion)R(eference)U(nit)s, capable of measuring the six degrees of freedom of an unconstrained frame are therefore widely employed. Since the payload transfer can be reduced to a tool point control task the goal of the heave compensation will be to minimize the deviation of the position and/or velocity of the tool point relative to reference values.

The tool point can be a hook that a hanging load is attached to, or it can be a gripper tool for transporting objects but quite often the payload will be connected to the end point of the manipulator as a pendulum via an non-actuated spherical, universal or revolute joint.

This work has been partially funded by NORCOWE under grant 193821/S60 from the Research Council of Norway. NORCOWE is a consortium with partners from industry and science, hosted by Christian Michelsen Research.

Tool point control for a non-redundant manipulator is done by calculation of the inverse kinematics. This gives a solution for what position the joints must be in, based on a given tool point. Inverse kinematic control for hydraulically or electrically actuated machines has been done by [8] and [6]. Approaches for solving the joint position for a given tool point position for a redundant manipulator is proposed in [18] and [5]. As an advantage the redundancy also gives the opportunities to optimize properties for the manipulator by controlling the null space motion of the manipulator. Work has been done to find optimization functions that can increase performance by controlling the null space motion. An approach by [16] has been minimization of restoring moments in [1] where a redundant manipulator was used to compensate motion caused by waves found in the North Sea.

In this paper we put forward a method for tool point control of a planar manipulator with redundant hydraulic actuation and a payload hanging from an unactuated revolute joint. The method is implemented both numerically and experimentally on a down-scaled version of a typical loader crane. Similar work where a pendulum is stabilized using Linear Quadratic Regulator (LQR) has been done by [17] and [3].

2. CONSIDERED SYSTEM

In this paper emphasis is on tracking i.e., tracking the tool point path in the global coordinate system while minimizing the oscillation of the pendulum, see Fig. 1. The position vector $\mathbf{x}$ is defined as the vector from point O to point P measured in the local coordinate system:

$$\mathbf{x} = \begin{bmatrix} x_{P1}^{(L)} \\ x_{P2}^{(L)} \end{bmatrix} \tag{1}$$

In the experimental tests the Stewart platform moves in reference to a sinewave in the vertical direction. The distance from the ground to the platform is defined as $z(t)$

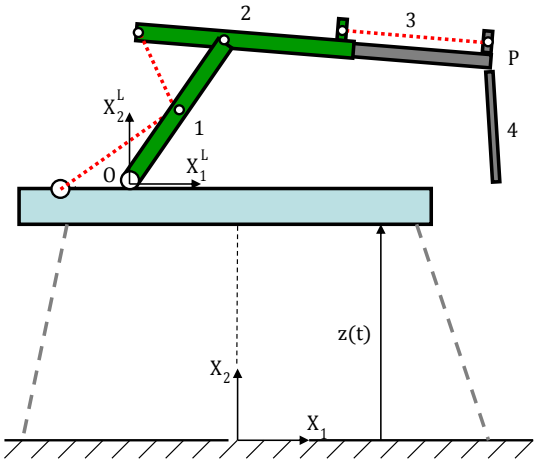

Fig. 1 *Manipulator with four links.*

and its time derivative $\dot{z}(t)$, see Fig. 1. The redundant manipulator is installed on top of a Stewart platform as shown in Fig. 1.

The redundant manipulator investigated in this paper is a four-bar mechanism. It consists of three rotational (q_1, q_2, q_4) and one prismatic joint (q_3) as shown in Fig. 2. Each joint except q_4 is actuated by a hydraulic cylinder controlled by a servo valve. The two actuated rotational joint angles are measured using quadrature encoders, and the prismatic joint is measured using a linear potentiometer. The unactuated joint q_4 connects the pendulum (link 4) with the telescopic link 3, see Fig. 2. The angle of the fourth bar, q_4 is measured using an inertial measurement unit consisting of a gyroscope and an accelerometer, where the angle of the pendulum is measured in reference to the earth gravity. This gives an advantage when it comes to stabilizing the pendulum since the stable point is parallel to the gravitational field.

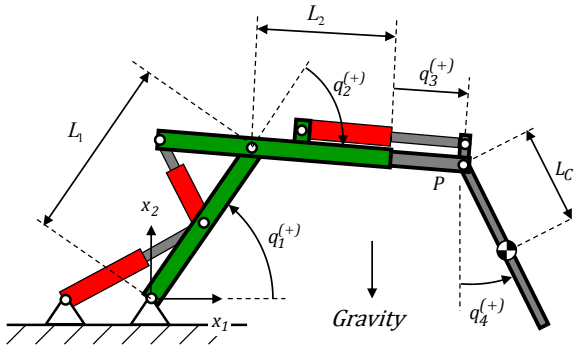

Fig. 2 *Kinematic structure of the redundant manipulator showing the joint variables and link lengths.*

2.1 Kinematics

The structure of the investigated manipulator is shown in Fig. 2, where L_1 and L_2 are the link lengths and joint position q_3 is a translation of the 3rd link relative to the 2nd link. The distance to the center of mass of the fourth link relative to the tool point P is denoted as L_c. The forward kinematics of the considered manipulator describes position vector eq. eq. (1) based on the joints position as follows:

$$x_{P1}^{(L)} = L_1 \cos(q_1) + (L_2 + q_3)\cos(q_1 - q_2) \quad (2)$$

$$x_{P2}^{(L)} = L_1 \sin(q_1) + (L_2 + q_3)\sin(q_1 - q_2) \quad (3)$$

For a manipulator containing n links the kinematics is written as follows:

$$\mathbf{x} = f(\mathbf{q}) \quad (4)$$

$$\dot{\mathbf{x}} = \mathbf{J}(\mathbf{q})\dot{\mathbf{q}} \quad (5)$$

where $\mathbf{x} \in R^m (n > m)$ is the position coordinates of the end-point with m degrees of freedom, and $\dot{\mathbf{x}}$ is the end-point velocity which is normally prescribed in tracking and planned path operations. The vector $\mathbf{q} \in R^n$ is the joint position and $\dot{\mathbf{q}}$ is the joint velocity, $\mathbf{J}(\mathbf{q}) \in R^{m \times n}$ is the Jacobian matrix defined as:

$$\mathbf{J} = \frac{\partial \mathbf{f}(\mathbf{q})}{\partial \mathbf{q}} \quad (6)$$

The Jacobian matrix of a redundant manipulator is non-square and not invertible, hence the pseudo-inverse of the Jacobian $(\mathbf{J}^\dagger)$ is used as in [12].

$$\mathbf{J}^\dagger = \mathbf{J}^\mathbf{T}(\mathbf{J}\mathbf{J}^\mathbf{T})^{-\mathbf{1}} \quad (7)$$

Using the pseudo-inverse Jacobian, the relation between the joint and tool point velocities of the redundant manipulator is written as follows:

$$\dot{\mathbf{q}} = \mathbf{J}^\dagger(\mathbf{q})\dot{\mathbf{x}} \quad (8)$$

Computing the joint velocities according to eq. eq. (8) corresponds to choosing the set of joint velocities that minimizes $\frac{1}{2}\dot{\mathbf{q}}^T\dot{\mathbf{q}}$ while meeting the end-point velocity constraint.

2.2 Weighting Matrix

The matrix $\mathbf{W} \in \mathbf{R}^{\mathbf{n}\times\mathbf{n}}$ is a positive diagonal matrix and contains a weighting of each of the joint velocities.

$$\mathbf{W} = \begin{bmatrix} W_1 & 0 & 0 \\ 0 & W_2 & 0 \\ 0 & 0 & W_3 \end{bmatrix} \quad (9)$$

The weighting matrix $\mathbf{W}$, see [7], is introduced so that the redundancy is handled by minimizing $\frac{1}{2}\dot{\mathbf{q}}^T\mathbf{W}\dot{\mathbf{q}}$. This makes it possible to take into account the velocity limits of each joint. In this paper the following weighting is used:

$$W_i = \frac{1}{(v_i^U - v_i^L)^2}, \quad i = 1..3 \quad (10)$$

where v_i^U and v_i^L are the upper and lower velocity limits of each joint respectively. A joint with a low velocity range will have a lower velocity reference during operation. Using the weighting matrix with pseudo-inverse Jacobian in eq. eq. (8), the following expression is obtained for the weighed pseudo-inverse Jacobian,

$$\mathbf{J}_\mathbf{W}^\dagger = \mathbf{W}^{-\mathbf{1}}\mathbf{J}^\mathbf{T}(\mathbf{J}\mathbf{W}^{-\mathbf{1}}\mathbf{J}^\mathbf{T})^{-\mathbf{1}} \quad (11)$$

A more general solution of eq. eq. (8) is presented by eq. eq. (12), where the weighted Pseudo-inverse Jacobian is used, see for example [13].

$$\dot{\mathbf{q}}_{\mathbf{W}} = \mathbf{J}_{\mathbf{W}}^{\dagger}\dot{\mathbf{x}} + (\mathbf{I} - \mathbf{J}_{\mathbf{W}}^{\dagger}\mathbf{J})\dot{\mathbf{q}}_{\mathbf{0}} \tag{12}$$

where $\mathbf{I} \in \mathbf{R}^{\mathbf{n}\times\mathbf{n}}$ is the identity matrix and $\dot{\mathbf{q}}_0 \in R^n$ is an arbitrary joint velocity vector. In eq. eq. (12) the null space mapping is introduced. The term $(\mathbf{I}-\mathbf{J}_{\mathbf{W}}^{\dagger}\mathbf{J})\dot{\mathbf{q}}_{\mathbf{0}}$ produces only a joint self-motion of the structure, but no task space motion.

2.3 Null Space

A widely adopted approach is to solve the null space redundancy by optimizing the scalar cost function $h(\mathbf{q})$ using the gradient projection method, choosing $\dot{\mathbf{q}}_{\mathbf{0}}$ to be the derivative of the cost function with regards to the joints.

$$\dot{\mathbf{q}}_0 = \frac{\partial h(\mathbf{q})}{\partial \mathbf{q}} \tag{13}$$

The cost function eq. eq. (14) was introduced by [14] and used in [11] and [15]. The main goal of the cost function is to avoid mechanical joint saturation.

$$h(\mathbf{q}) = \frac{1}{3}\sum_{i=1}^{i=3}\left(\frac{q_i - a_i}{a_i - y_i^U}\right)^2 \tag{14}$$

$$a_i = \frac{y_i^U + y_i^L}{2} \tag{15}$$

where y_i^U and y_i^L are the upper and lower position limits for each joint respectively.

2.4 Hydraulic System

The governing steady state equation for the hydraulic actuated cylinder are described by eqs. (16-18).

$$Q_i = A_i \cdot v_i \tag{16}$$

$$Q_i = Q_{N,i} \cdot u_i \cdot sign(\Delta p_i) \cdot \sqrt{\frac{|\Delta p_i|}{\Delta p_{N,i}}} \tag{17}$$

$$\Delta p_i = \left\{ \begin{array}{ll} p_s - p_i, & u_i \geq 0 \\ p_i, & u_i < 0 \end{array} \right\} \tag{18}$$

In eq. eq. (16-18) $i = 1...3$ is the circuit index, see Fig. 3. Furthermore, p_s is the constant supply pressure, Q is the volume flow and A is the piston area. The servo valve is modeled as a sharp edged orifice based on nominal parameters, where the nominal volume flow Q_N is measured at nominal pressure drop Δp_N across the orifice with the valve fully opened. The spool travel $-1 \leq u \leq 1$ is the controlled variable of the valve. Based on the equations above it is possible to compute a spool position from the cylinder velocities if the pressure drop is known, see [2]. The hydraulic circuit in Fig. 3 shows the connection of the servo valves and cylinders. Rearranging eq. (17) yields:

$$u_i = \frac{A_i \cdot v_i}{Q_{N,i}}\sqrt{\frac{\Delta p_{N,i}}{|\Delta p_i|}} \tag{19}$$

This equation is used as a forward coupling term, $\mathbf{D}(\mathbf{p})$, as shown in Fig. 4 such as:

$$\mathbf{u} = \mathbf{D}(\mathbf{p})\mathbf{v} \tag{20}$$

where $\mathbf{u}$ is the current signals for the servo valves and $\mathbf{p}$ is the oil pressures.

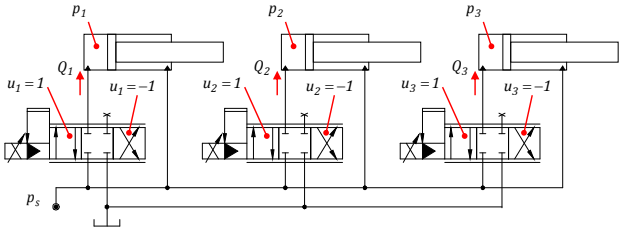

Fig. 3 *Hydraulic diagram of the manipulator. Note that the pressure side is directly connected to the piston side of every cylinder.*

3. CONTROL SCHEME

The motion control for the redundant manipulator is based on the pseudo-inverse Jacobian and the null-space vector. There is one actuator controller for each joint, and it uses the joint velocity reference to generate a current signal to the servo valve. The controller generates a joint velocity reference that is given to the actuator controller shown in Fig. 4. The block $\mathbf{C}(\mathbf{q})$ is the transformation matrix that transforms the angular velocity into linear cylinder velocity.

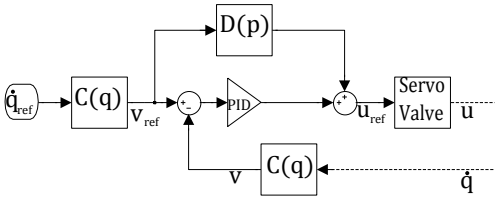

Fig. 4 *Actuator velocity control structure.*

3.0.1 Open and Closed Loop Velocity Control

There is an open loop controller that uses eq. (19) as a feed forward coupling to calculate the opening of the servo valve based on the velocity input reference and the pressure measurements. This equation handles the non-linearity of the valve and pressure levels described in [2]. The block $\mathbf{D}(\mathbf{p})$ represents the feed-forward coupling term shown in Fig. 4. A closed loop proportional-integral-derivative gain is used to correct any error left from the feed forward coupling term and shown as the PID block.

3.0.2 Tracking Control

The tool-point tracking controller for the redundant manipulator displayed in Fig. 5 shows the complete structure of the tool position and velocity set-points to the manipulator.

The fixed constants K_p and K_d are gains for minimizing both position and velocity errors. The matrix $\mathbf{J}_{\mathbf{W}}^{\dagger}(\mathbf{q})$ is the weighted pseudo inverse term in the first part of eq. (12), while $\mathbf{N}(\mathbf{q})$ represents the Null Space Control, and is the $(\mathbf{I} - \mathbf{J}_{\mathbf{W}}^{\dagger}\mathbf{J})\dot{\mathbf{q}}_{\mathbf{0}}$ term of eq. (12). $\mathbf{H}(\mathbf{q})$ is the actuator regulator and is described in Fig. 4. Blocks $\mathbf{J}(\mathbf{q})$ and $\mathbf{F}(\mathbf{q})$ represent Jacobian matrix and forward kinematics,

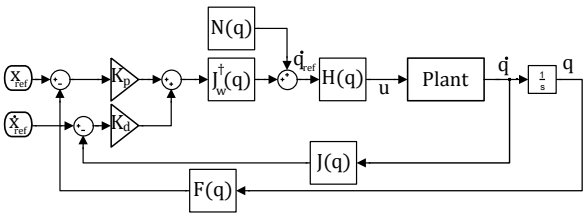

Fig. 5 *Manipulator tracking control structure.*

respectively.

3.1 LQR Pendulum Oscillation Compensation

The fourth bar of the manipulator can be considered as a hanging pendulum with no flexibility. The forces acting on the pendulum are caused by gravity and the motion of the point P. Using the free body diagram and the kinetic

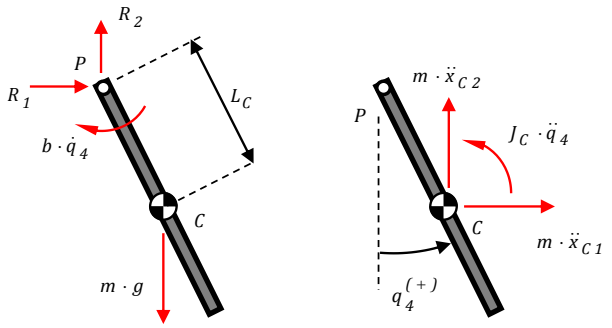

Fig. 6 *Free body diagram and kinetic diagram of fourth link.*

diagram of Fig. 6 we get the following relationship:

$$-b\dot{q}_4 - m_C g L_C \sin(q_4) = J_C \ddot{q}_4 + m_C \ddot{x}_{C2} L_C \sin(q_4) + m_C \ddot{x}_{C1} L_C \cos(q_4) \quad (21)$$

Introducing the kinematics constraints:

$$\ddot{x}_{C1} = \ddot{x}_{P1} + L_C \cos(q_4)\ddot{q}_4 - L_C \sin(q_4)\dot{q}_4^2 \quad (22)$$

$$\ddot{x}_{C2} = \ddot{x}_{P2} + L_C \sin(q_4)\ddot{q}_4 + L_C \cos(q_4)\dot{q}_4^2 \quad (23)$$

it is possible to set up an expression for the angular acceleration as function of the tool point accelerations:

$$\ddot{q}_4 = -\frac{1}{J_P}(b\dot{q}_4 + m_C g L_C \sin(q_4) + m_C \ddot{x}_{P2} L_C \sin(q_4) + m\ddot{x}_{P1} L_C \cos(q_4)) \quad (24)$$

where b is a damping coefficient, J_C and J_P are the mass moments of inertia of the pendulum with respect to the points C and P, respectively. In the experiments presented in this paper the motion of the Stewart platform, see Fig. 1, is restricted to purely vertical motion and therefore the correlation between global and local accelerations of point P simplifies to:

$$\ddot{x}_{P1} = \ddot{x}_{P1}^{(L)} \quad (25)$$

$$\ddot{x}_{P2} = \ddot{x}_{P2}^{(L)} + \ddot{z}(t) \quad (26)$$

Linearizing the equation around the stable equilibrium point $q_4 = 0$ is represented in state space by:

$$\dot{\mathbf{x}}_{ss}(t) = \mathbf{A}\mathbf{x}_{\mathbf{ss}}(\mathbf{t}) + \mathbf{B}\mathbf{i}_{\mathbf{ss}}(\mathbf{t}) \quad (27)$$

$$\mathbf{x}_{\mathbf{ss}}(\mathbf{t}) = \begin{bmatrix} q_4 & \dot{q}_4 \end{bmatrix}^T \quad (28)$$

$$\mathbf{A} = \begin{bmatrix} 0 & 1 \\ -\frac{m_C g L_C}{J_P} & -\frac{b}{J_P} \end{bmatrix} \quad (29)$$

$$\mathbf{B} = \begin{bmatrix} 0 & -\frac{m_C L_C}{J_P} \end{bmatrix}^T \quad (30)$$

where $i_{ss}(t) = \ddot{x}_{P1}$ is the external input and $\mathbf{x_{ss}}$ is the state space vector.

In order to stabilize the swinging pendulum while keeping the tool point at a relatively fixed position, LQR control is used. The well-known Riccati equation is solved to find the control gain matrix $\mathbf{K}(\mathbf{1} \times \mathbf{2})$ such as:

$$i_{ss} = -\mathbf{K}\mathbf{x}_{\mathbf{ss}} \quad (31)$$

The Riccati equation contains the matrix $\mathbf{Q}$ and the scalar R that are tuned with a view to get the best accuracy based on performance and actuator limits. The control effort from the oscillation compensation is simply integrated in the overall tracking controller of Fig. 5 by adding the integrated value of $i_s s$ to $\dot{x}_{ref}$:

$$\dot{x}_{ref} = \dot{x}_{ref}^{(TC)} + \int i_{ss} dt \quad (32)$$

where $\dot{x}_{ref}^{(TC)}$ is the reference velocity from the path planner (or operator-in-the-loop) associated with the tracking controller. One advantage of the proposed controller is the modular design. The PID-controller with velocity feedforward is commonly used in offshore applications. The fact that the LQR compensation controller can simply be added to the velocity reference is attractive from an implementation point of view.

4. EXPERIMENTAL RESULTS

The overall control structure combining the tracking control and the oscillation compensation has been implemented in practice. The physical test setup is shown in Fig. 7 and is desribed in more detail in [1]. Three different scenarios A, B and C have been investigated.

4.1 Disturbance Compensation

In this scenario the target of the tracking control is a fixed position for point P. In Fig. 8 the red line shows the oscillation of the pendulum without compensation, while the blue line shows the oscillation with compensation. The pendulum is dropped with zero initial velocity at an angle of 45 degrees. The green line represents the control signal and is the joint q_4 horizontal velocity represented by the right axis in Fig. 8. The curves clearly show that the uncompensated oscillation is subjected to some friction/damping and, simultaneously, it is obvious that the compensation actively brings the pendulum to its stable position.

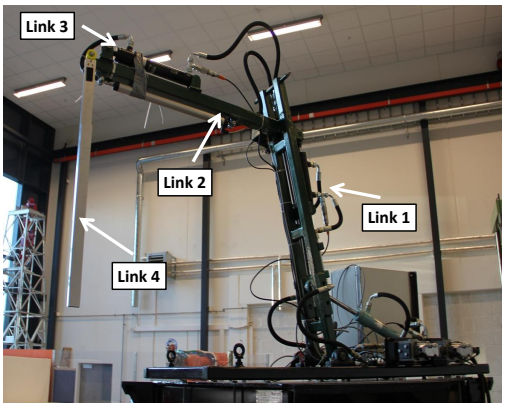

Fig. 7 *The redundant hydraulic manipulator used for experimental tests.*

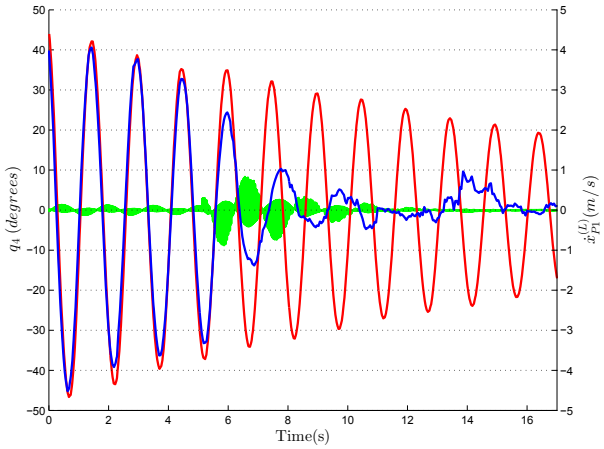

Fig. 8 *Free pendulum oscillations at joint q_4 with and without compensation.*

4.2 Tracking a Straight Line Trajectory

The tracking performance of the end-effector was evaluated experimentally by prescribing a straight line trajectory. The two experiments 1 and 2 is done with a different tracking trajectory. The reference position of the end-effector starts at $\mathbf{x}_{\mathbf{P_1,init}}^{(\mathbf{L})} = [\mathbf{1}, \mathbf{1}]^{\mathbf{T}}\ \mathbf{m}$ and moves to $\mathbf{x}_{\mathbf{P_1,final}}^{(\mathbf{L})} = [\mathbf{1.4}, \mathbf{0.7}]^{\mathbf{T}}\ \mathbf{m}$. In Figs. 9 and 10 the red lines indicate prescribed coordinates and the blue lines indicate the measured coordinates. The black line is the angle of the pendulum and it is clear that the oscillation compensation both reduces the peak value and the settling time for the pendulum angle during the tracking of the straight line.

4.3 Tracking Heave Compensation

In this scenario the Stewart platform is set in a sinusoidal vertical motion in order to introduce a heave disturbance. The amplitude and frequency of the motion is $0.15\ m$ and $0.2\ Hz$ respectively. The target of the tracking control is to maintain a constant position in the global coordinate system. Thereby, the local reference becomes the inverted motion of the platform. The results are shown in Fig. 11 and it is evident that the compensation is capable of removing any pendulum oscillations even when subjected to continuous disturbance.

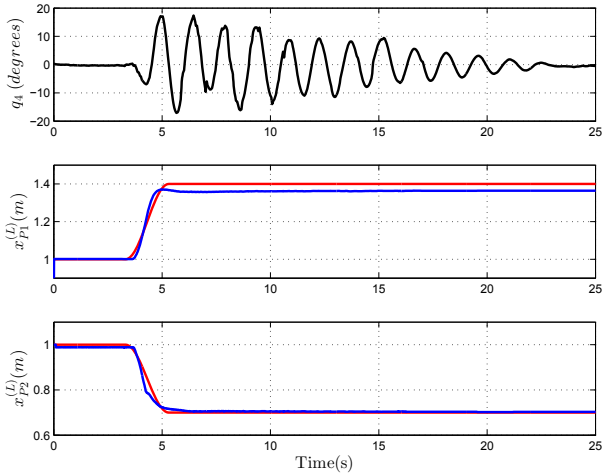

Fig. 9 *Tracking of end-effector without compensation in experiment 1.*

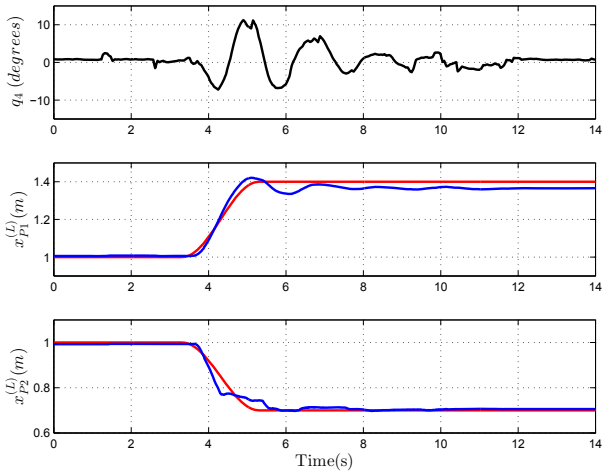

Fig. 10 *Tracking of end effector with compensation in experiment 1.*

5. DISCUSSION AND CONCLUSIONS

In this paper a method for tool point control of a four degree-of-freedom mechanical manipulator is presented both theoretically and experimentally. The manipulator and the associated tool point control are developed with a view to be used in offshore applications for payload transfer. Because of this the manipulator is designed with some typical characteristics: hydraulic actuation, redundant actuation and a free swinging payload. Similarly, the control scheme has been developed to handle: avoidance of saturation of the linear actuators, avoidance of saturation of the servo valves, ability of the tool point of the manipulator to track a path and the ability of the manipulator to dampen out oscillations in the non-actuated degree of freedom even under continuous disturbance from wave induced heave motion. The control scheme is unique in the way that it addresses all of the above character-

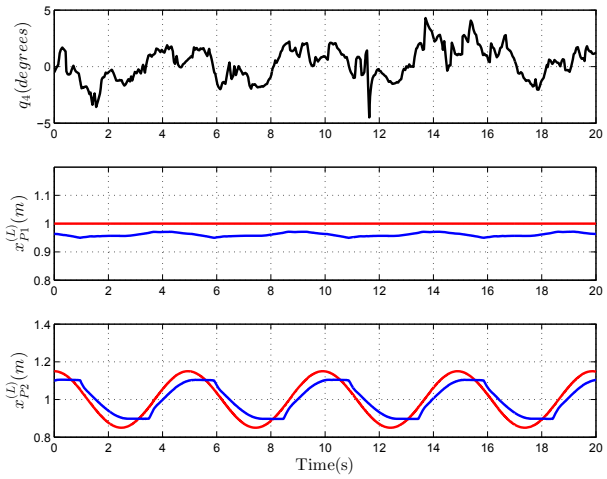

Fig. 11 *Tracking of end effector with heave motion and compensation.*

istics of both the manipulator and the operational scenarios. The control scheme has been implemented in practice and been shown to work as expected but has not been subjected to any kind of optimization or fine tuning since this is considered to lie outside the scope of the current paper. In future work the control scheme is to be implemented on a commercial vehicle loader crane with a view to, eventually, apply the scheme in actual offshore conditions.

REFERENCES

[1] M.B. Kjelland, I. Tyapin, G. Hovland and M.R. Hansen, Tool-Point Control for a Redundant Heave Compensated Hydraulic Actuator," *Proc. IFAC Workshop on Automatic Control in Offshore Oil and Gas Production, Trondheim*, 2012

[2] Qin Zhang, Hydraulic linear actuator velocity control using a feedforward-plus-PID control," *Int. J. Flexible Automation and Integrated Manufacturing 7*, pp. 277-292, 2000.

[3] Chunhacha, P. and Benjanarasuth, T., Parameters tuning effects in the model predictive control of an inverted pendulum," *TENCON 2011 - 2011 IEEE Region 10 Conference*, pp. 1080-1084, 2011.

[4] Z. Peng and N. Kessissoglou, An Integrated Approach to Fault Diagnosis of Machinery Using Wear Debris and Vibration Analysis," *Wear*, pp. 1221-1232, vol.255, num. 7-12, 2003.

[5] Jonghoon Park and Youngjin Choi and Wan Kyun Chung and Youngil Youm, Multiple tasks kinematics using weighted pseudo-inverse for kinematically redundant manipulators," *Robotics and Automation, 2001. Proceedings 2001 ICRA. IEEE International Conference on*, pp. 4041-4047, vol.4, num. 7-12, 2001.

[6] Kucuk, S. and Bingul, Z., The inverse kinematics solutions of industrial robot manipulators," *Mechatronics, 2004. ICM '04. Proceedings of the IEEE International Conference on*, pp. 274-279, 2004.

[7] Jonghoon Park and WanKyun Chung and Youngil Youm, Weighted decomposition of kinematics and dynamics of kinematically redundant manipulators," *Robotics and Automation, 1996. Proceedings., 1996 IEEE International Conference on*, pp. 480-486, vol.1, 1996.

[8] Cinkelj, J. and Kamnik, R. and Cepon, P. and Mihelj, M. and Munih, M., Robotic control system for hydraulic telescopic handler," *Robotics in Alpe-Adria-Danube Region (RAAD), 2010 IEEE 19th International Workshop on*, pp. 137-142, vol.1, 2010.

[9] Min-Jie Liu and Cong-Xin Li and Chong-Ni Li, Dynamics analysis of the Gough-Stewart platform manipulator," *Robotics and Automation, IEEE Transactions on*, pp. 94-98, vol. 16, num. 1, 2000.

[10] Liu, K. and Fitzgerald, J.M. and Lewis, F.L., Kinematic analysis of a Stewart platform manipulator," *Industrial Electronics, IEEE Transactions on*, pp. 282-293, vol. 40, num. 2, 1993.

[11] Mikkel M. Pedersen and Michael R. Hansen and Morten Ballebye, Developing a Tool Point Control Scheme for a Hydraulic Crane Using Interactive Real-time Dynamic Simulation," *Modeling, Identification and Control*, pp. 133-143, vol. 31, num. 4, 2010.

[12] Daniel E. Whitney, Resolved Motion Rate Control of Manipulators and Human Prostheses," *IEEE Trans. Man-Machine Systems*, pp. 47-53, vol. 10, 1969.

[13] Bruno Siciliano, Kinematic Control of Redundant Robot Manipulators: A Tutorial," *Journal of Intelligent and Robotic Systems*, pp. 201-212, vol. 3, 1990.

[14] A. Ligeois, Automatic supervisory control of the configuration and behavior of multibody mechanisms," *IEEE Trans. Systems Man Cybernet*, pp. 868-871, vol. 7, 1977.

[15] Chan, T. F. and Dubey, Weighted least-norm solution based scheme for avoiding joint limits for redundant manipulators," *Robotics and Automation*, pp. 395-402, vol. 3, 1993.

[16] Jonghui Han and Wan Kyun Chung, Redundancy resolution for underwater vehicle-manipulator systems with minimizing restoring moments," *Intelligent Robots and Systems, 2007. IROS 2007. IEEE/RSJ International Conference on*, pp. 3522-3527, 2007.

[17] Wen, B. and Homaifar, A. and Bikdash, M. and Kimiaghalam, B., Modeling and optimal control design of shipboard crane," *American Control Conference, 1999. Proceedings of the 1999*, pp. 593-597, vol. 1, 1999.

[18] Beiner, L. and Mattila, An improved pseudoinverse solution for redundant hydraulic manipulators," *Robotica*, pp. 173179, vol. 17, 1999.